

## On the stability of the $\pi$ -allyl intermediate in molybdenum-catalyzed asymmetric alkylations

Jennifer A. R. Luft,<sup>a</sup> Zhi-Xiang Yu,<sup>a,†</sup> David L. Hughes,<sup>b</sup> Guy C. Lloyd-Jones,<sup>c</sup> Shane W. Krska<sup>b</sup> and Kendall N. Houk<sup>a,\*</sup>

<sup>a</sup>Department of Chemistry and Biochemistry, University of California, Los Angeles, CA 90095, USA

<sup>b</sup>Merck Research Laboratories, Merck and Co., Inc., Rahway, NJ 07065, USA

<sup>c</sup>School of Chemistry, University of Bristol, Bristol BS8 ITS, United Kingdom

Received 5 January 2006; accepted 28 January 2006

Available online 20 March 2006

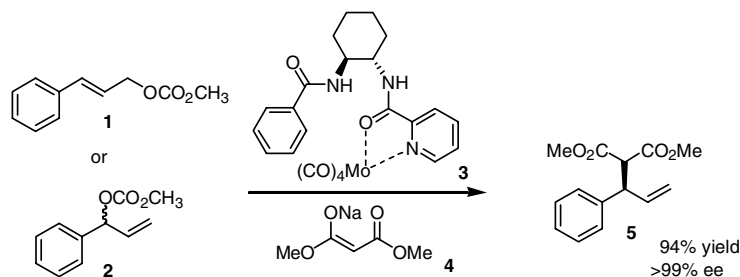
**Abstract**—Density functional theory calculations were performed on the apparent  $\eta^3$ - $\pi$ -allyl molybdenum intermediate that is observed during molybdenum-catalyzed asymmetric allylation [*Proc. Natl. Acad. Sci. U.S.A.* **2004**, *101*, 5379]. The relative stabilities of geometric isomers, diastereoisomers, and  $\pi$ -allyl rotamers of the  $\pi$ -allyl molybdenum intermediate were investigated. Calculations show that the observed intermediate is the most stable because of two factors: (1) the observed  $\pi$ -allyl molybdenum intermediate maximizes the bonding and back-bonding interactions between molybdenum and the  $\pi$ -allyl ligand; and (2) the observed  $\pi$ -allyl molybdenum intermediate minimizes the steric interactions between the chiral ligand and the  $\pi$ -allyl group.  
© 2006 Elsevier Ltd. All rights reserved.

### 1. Introduction

Metal-catalyzed asymmetric allylations have become a useful synthetic method.<sup>1</sup> Early work focused on palladium complexes, but these reactions generally give achiral, linear products from asymmetric substrates. Certain ligands have been found that induce the formation of branched products with reasonable regioselectivity and enantioselectivity.<sup>2</sup> Other transition metal, ligand com-

binations have been developed to provide branched products, using Ru, Rh, Ir, Fe, and W.<sup>3</sup>

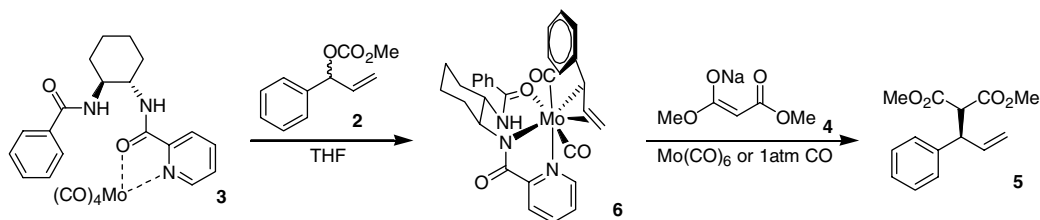
Molybdenum is commonly used for branched regioselectivity. Molybdenum-catalyzed allylations afford branched products in high yield, enantioselectivity, and regioselectivity from either linear or branched substrates (Scheme 1). Molybdenum allylations occur with the loss of substrate stereochemistry.<sup>4</sup> Oxidative



**Scheme 1.** Molybdenum complex 3 reacts with linear or branched substrates 1 or 2 to give allylated product 5 with high regioselectivity and enantioselectivity.

\* Corresponding author. Tel.: +1 310 206 0515; fax: +1 310 206 1843; e-mail: houk@chem.ucla.edu

† Key Laboratory of Bioorganic Chemistry and Molecular Engineering of Ministry of Education, College of Chemistry, Peking University, Beijing 100871, China.



**Scheme 2.** Molybdenum complex **3** reacts with branched or linear substrates to give allylated product **5** via a single  $\pi$ -allyl complex, **6**.

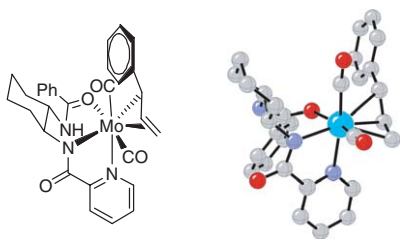


**Figure 1.** X-ray crystal structure of **6**.<sup>6</sup>

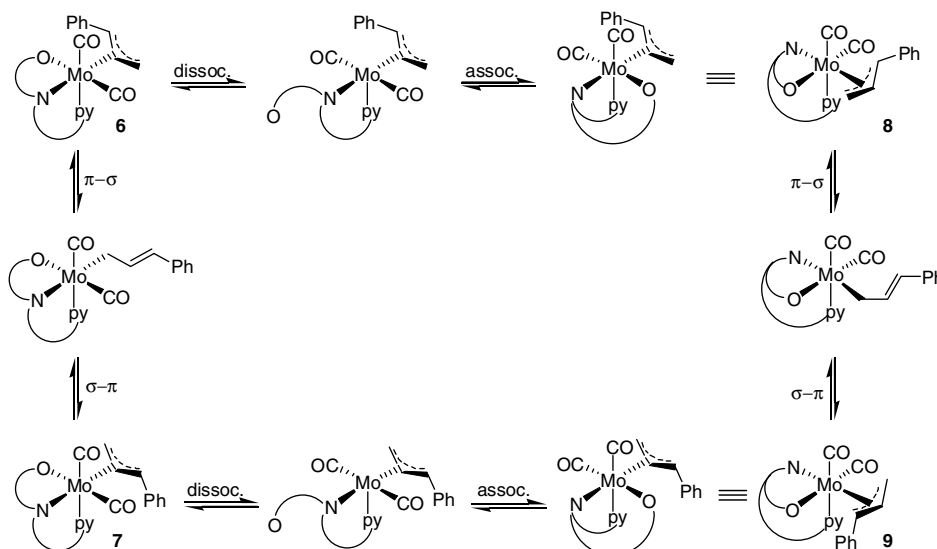
addition and nucleophilic displacement have been shown to occur with retention of configuration.<sup>5</sup>

Stoichiometric reaction of the molybdenum complex **3** with branched substrate **2** led to the formation of **6** (Scheme 2).<sup>4</sup> A crystal of **6** was grown, and the X-ray structure is shown in Figure 1. The crystal structure agrees with the solution structure determined from NMR spectroscopy. Exposure of **6** to nucleophile, **4**, with excess CO yields **5** in high yield, enantioselectivity, and regioselectivity.<sup>6</sup>

The crystal structure of **6** shows an eight-coordinate, 18-electron molybdenum complex. Compound **6** is octahedral, if the  $\pi$ -allyl ligand is considered as a single two-electron ligand. In an ideal octahedral complex,

$90^\circ$  separate the nearest ligands. Angles in **6** average  $90^\circ$ , but deviate from the ideal by as much as  $17^\circ$ . Two CO ligands surround the molybdenum center. The allyl moiety binds to molybdenum in something between an  $\eta^2$  and an  $\eta^3$  fashion (distances of 2.456, 2.220, and 2.300 for the  $\alpha$ -,  $\beta$ -, and  $\gamma$ -carbons, respectively). The chiral ligand binds molybdenum through the pyridine nitrogen, the deprotonated picolinamide nitrogen, and the benzamide oxygen. The  $\pi$ -allyl ligand is *trans* to the picolinamide nitrogen and *cis* to the benzamide oxygen and pyridine nitrogen. The CO ligands are *trans* to the benzamide oxygen and the pyridine nitrogen.

Previous publications have illustrated that the NMR data for **6** in solution also fits its pseudo-enantiomer, **9**, wherein the stereochemistry at the molybdenum center has been reversed, but maintenance of the chiral ligand stereochemistries causes **6** and **9** to actually be diastereomers. Isomers **6** and **9** could interconvert through dissociation–association of the ligand (shown horizontally in Scheme 3) in conjunction with  $\pi$ – $\sigma$ – $\pi$  isomerization (shown vertically, Scheme 3). Neither **7** nor **8** were detected via NMR.<sup>7</sup> One of these isomers could be a key intermediate in the catalytic cycle, since catalytic flux often proceeds through a minor stereoisomer.<sup>8</sup>



**Scheme 3.** Molybdenum complex **6** may rearrange via  $\pi$ – $\sigma$ – $\pi$  isomerization (shown vertically) or dissociation, association of the ligand (shown horizontally) to **7**, **8**, or **9**.

## 2. Results and discussion

We have investigated as to why **6** is more stable than other stereoisomers of this intermediate. Density functional theory calculations were used to compute the relative energies of plausible isomers, and to determine the origin of the preference for **6**.

Density functional theory has been shown to be an effective method for modeling organometallic compounds<sup>9</sup> including those with molybdenum.<sup>10</sup> Geometric isomers, diastereoisomers and  $\pi$ -allyl rotamers of **6** were optimized using ab initio and DFT methods. DFT energies are discussed here.

The calculated structure of **6** is shown in Figure 2. A comparison of distances and angles for the X-ray structure and the calculated structure is given in Table 1. Calculated bond distances are within 0.15 Å of the observed, with a mean absolute deviation of 0.005 Å. Differences in angles average 1.1° and the largest discrepancy is in the pyridine–molybdenum–carbonyl angle (97.9° vs 95.5°).

Molybdenum binds the  $\beta$  and  $\gamma$  carbons in an  $\eta^2$  fashion, with a weaker interaction between the  $\alpha$ -carbon and molybdenum. Steric interactions and cation stabilization by the phenyl group cause the elongation of the Mo–C3 bond. Distances in **6**<sub>exp</sub> and **6**<sub>calcd</sub> are within 0.8 Å of previously reported Mo– $\eta^3$ -1-phenylallyl dis-

tances.<sup>11</sup> Elongation of the molybdenum– $\alpha$  carbon bond is observed in substituted  $\eta^3$  complexes,<sup>12</sup> with one exception.<sup>12a</sup> Previous publications indicate that molybdenum binds unsubstituted allyl groups symmetrically.<sup>13</sup> Geometry optimizations of Mo(CO)<sub>2</sub>(lig)( $\eta^3$ -C<sub>3</sub>H<sub>5</sub>) gave symmetric Mo-allyl distances, confirming that the phenyl ring in **6** produces unsymmetrical binding.

Molecular orbitals of octahedral complexes are formed by combining the empty s, p<sub>x</sub>, p<sub>y</sub>, p<sub>z</sub>, d<sub>z<sup>2</sup></sub>, and d<sub>x<sup>2</sup>-y<sup>2</sup></sub> orbitals of the metal center (or linear combinations thereof) with filled valence orbitals of the ligands. The filled d<sub>xy</sub>, d<sub>xz</sub>, and d<sub>yz</sub> orbitals are reserved for backbonding with empty ligand  $\pi^*$  orbitals.<sup>14</sup> In **6**, molybdenum binds the  $\pi$ -allyl ligand through a predominately d<sub>z<sup>2</sup></sub> orbital,<sup>15</sup> Figure 3. The equatorial lobe of the hybridized orbital overlaps with the  $\pi$  orbital, while the center lobe overlaps with the  $\alpha$ -carbon of the allyl ligand.

Mo(CO)<sub>2</sub>(lig)( $\eta^3$ -CH<sub>2</sub>CHCHPh) has three ligands that have low-lying, empty orbitals that may participate in backbonding; two carbonyl  $\pi^*$  orbitals, and one allyl  $\pi^*$  orbital. Backbonding is maximized when these three ligands are *cis* on the octahedral complex so that each ligand may backbond with one of the filled, orthogonal d orbitals.<sup>12a,16</sup> X-ray structures of octahedral Mo( $\eta^3$ -allyl)(CO)<sub>2</sub>L<sub>3</sub> complexes confirm that the allyl group and carbonyl ligands prefer to reside *cis*,<sup>12,13</sup> unless steric interactions between ligands are prohibitive.<sup>17</sup>

The ligand discussed herein is tridentate. Steric constraints in the ligand force the ligand to bind molybdenum facially. Therefore, all complexes of Mo(CO)<sub>2</sub>(lig)( $\eta^3$ -CH<sub>2</sub>CHCHPh) place the three backbonding ligands *cis*, as is preferred. Molybdenum may bind the ligand facially in two ways (Fig. 4). The two arrangements are pseudo-enantiomeric; they are enantiomers except for the cyclohexyl chirality, which does not change. Both pseudo-enantiomeric binding modes were investigated. The ligand as found in **6** is preferred because the benzamide phenyl ring is positioned out of the equatorial plane. In the pseudo-enantiomeric orientation, the benzamide phenyl ring lies in the equatorial plane, increasing steric interactions in this plane.

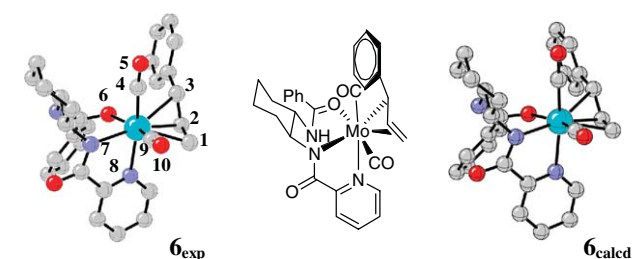


Figure 2. Experimental and calculated structures of **6**.

Table 1. Distances (Å) and angles (°) in **6**<sub>exp</sub> and **6**<sub>calcd</sub>

Dist./angle	<b>6</b> <sub>exp</sub>	<b>6</b> <sub>calcd</sub>
Mo–C1	2.300 Å	2.32 Å
Mo–C2	2.220 Å	2.29 Å
Mo–C3	2.456 Å	2.54 Å
Mo–C4	1.936 Å	1.95 Å
C4–O5	1.152 Å	1.17 Å
Mo–O6	2.201 Å	2.33 Å
Mo–N7	2.171 Å	2.20 Å
Mo–N8	2.280 Å	2.36 Å
Mo–C9	1.936 Å	1.97 Å
∠C1–Mo–C2	36.6°	36.1°
∠C2–Mo–C3	34.8°	33.2°
∠C2–Mo–C4	100.7°	101.4°
∠C4–Mo–O6	96.9°	95.7°
∠O6–Mo–N7	76.2°	77.2°
∠N7–Mo–N8	72.5°	73.2°
∠N8–Mo–C9	97.9°	95.5°
∠C9–Mo–C1	68.3°	69.3°

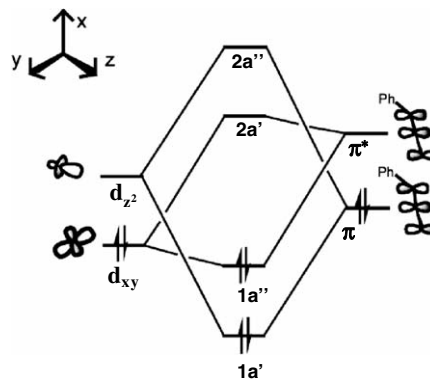


Figure 3. Extended Hückel molecular orbital (EHMO) energy level diagram for the interaction of the Mo(lig)(CO)<sub>2</sub> fragment orbitals with the allyl fragment orbitals.

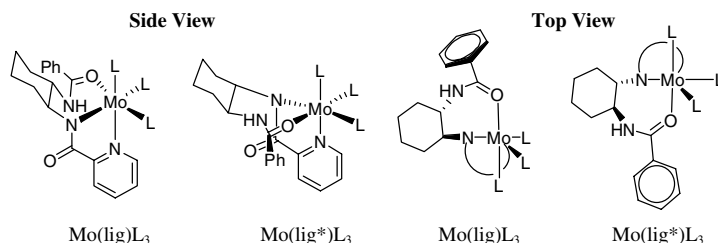


Figure 4. Two views of the potential orientations of the chiral ligand around the molybdenum center.

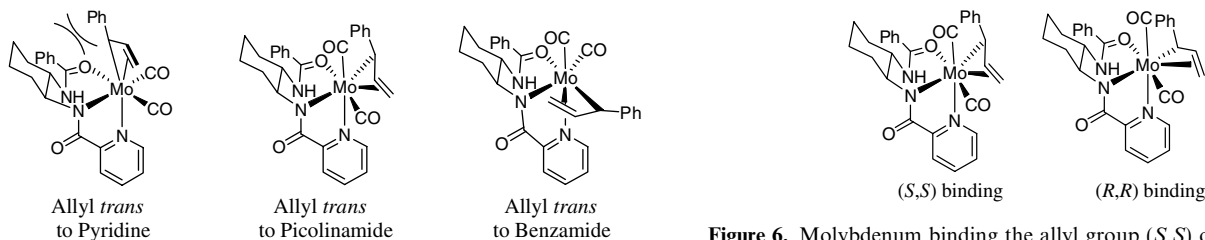


Figure 5. Allyl group placements around the molybdenum center.

Since molybdenum binds the ligand facially, there are three possible locations for the allyl group: allyl *trans* to the pyridine nitrogen; allyl *trans* to the picolinamide nitrogen; and allyl *trans* to the benzamide oxygen, Figure 5. Allyl *trans* to the picolinamide nitrogen is preferred for steric and electronic reasons. Allyl *trans* to pyridine increases the steric interactions between the cyclohexyl ring and the allyl group, destabilizing such isomers. Allyl *trans* to benzamide or picolinamide occasionally results in steric interactions with the ligand.

Electronically, the allyl *trans* to picolinamide is more stable than the allyl *trans* to pyridine or benzamide. The picolinamide nitrogen is deprotonated and has two orthogonal lone pairs. One lone pair forms a  $\sigma$  bond with molybdenum. The other lone pair is oriented to donate electron density into the molybdenum pseudo- $d_{xy}$  orbital, Figure 3, and increase backbonding between this orbital and the empty  $\pi^*$  orbital of the allyl group. This interaction stabilizes **6**. The benzamide oxygen and pyridine nitrogen are not  $\pi$  donating ligands and cannot increase the backbonding between molybdenum and the allyl ligand.

Complexes with allyl *trans* to picolinamide are more stable. Since the allyl group is unsymmetric, there are two prochiral faces that the molybdenum may bind. Literature examples of substituted allyl complexes show no overarching preference for binding of one face over the other.<sup>14</sup> Rather, the facial binding preference appears to be dependent on the complex. In this example, allyl bound (*S,S*) fits ideally into the pocket created by the chiral ligand and the two carbonyl ligands (Fig. 6). The substituted terminus is placed near the large benzamide, but is oriented out of the equatorial plane minimizing any destabilizing steric interactions. Binding the allyl (*R,R*) increases steric interactions with the benzamide group, elongating the Mo-allyl bonds and destabilizing the complex.

Finally, the allyl ligand may rotate about the molybdenum center. Previous investigations into  $\text{Mo}(\text{CO})_2(\eta^3\text{-allyl})\text{L}_3$  complexes show that the rotamers of the form **A** are strongly favored.<sup>12,13,18</sup> Crystal structures of  $\eta^3\text{-allyl}$  complexes always orientate the open face of the allyl toward the two carbonyl ligands. This preference is caused by interactions between filled molecular orbital of  $\text{Mo}(\text{CO})_2(\eta^3\text{-allyl})\text{L}_3$  complexes.<sup>16</sup> The filled allyl orbital interacts with the filled pseudo- $d_{xy}$  orbital, destabilizing the complex. This overlap is minimized when the open face of the allyl group points toward the carbonyl ligands: the terminal carbons overlies the  $\delta$  orbital equally and negate each other. Contact is maximized upon allyl rotation of  $180^\circ$ , where the  $\beta$  carbon overlaps the  $\delta$  orbital (Fig. 7). Orienting the allyl group as seen in **6** minimizes this overlap and is the most stable arrangement.

A combination of steric and electronic factors make **6** the most stable dicarbonyl structure: the binding preference of the ligand; placing the  $\pi$ -allyl ligand *trans* to the picolinamide nitrogen; binding the allyl ligand (*S,S*); and orienting the allyl group such that it is open to the carbonyl ligands. All possible isomers with alternative arrangements were investigated. Isomers that lie

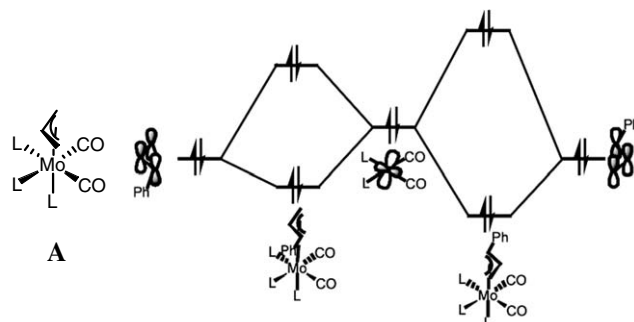


Figure 7. Molecular orbital analysis of rotamers of  $\text{Mo}(\text{CO})_2(\eta^3\text{-allyl})\text{L}_3$ .

within 10 kcal/mol of **6** are discussed here. Information on the other isomers is available in supporting information.

Rotation of the  $\pi$ -allyl group around the molybdenum center was explored. The  $\pi$ -allyl ligand of **6** was rotated by  $90^\circ$  increments and the resulting structures optimized. Results are shown in Figure 8. Molybdenum consistently binds the  $\beta$  and  $\gamma$  carbons of the  $\pi$ -allyl ligand in an  $\eta^2$  fashion for all isomers investigated. The rotamer with  $\pi$ -allyl phenyl apical optimized to either **6** or **10** during HF optimizations due to destabilizing electronic interactions between the phenyl  $\pi$  orbitals and the carbonyl  $\pi$  orbitals. In **10** (+7.2 kcal/mol), phenyl is proximal to the equatorial carbonyl ligand. Rotamer **11** (9.0 kcal/mol above **6**) orients phenyl basal and proximal to pyridine.

Rotamers of **6** are less stable than **6**, as was predicted. The overlap between the filled allyl orbital and the filled pseudo- $d_{xy}$  orbital is minimized in **6**. Contact is maximized upon allyl rotation of  $180^\circ$ . Isomers **10** and **11** both orient the allyl group such that the open face points away from the carbonyl ligands, which is destabilizing. Rotamer **11** is further destabilized by steric interactions between the allyl phenyl ring and pyridine.

Isomers **7**, **8**, and **9** formed via ligand dissociation–association and/or  $\pi$ – $\sigma$ – $\pi$  isomerization were investigated. The lowest energy rotamers of **7**, **8**, and **9** are shown in Figure 9. Details on higher energy rotamers are given

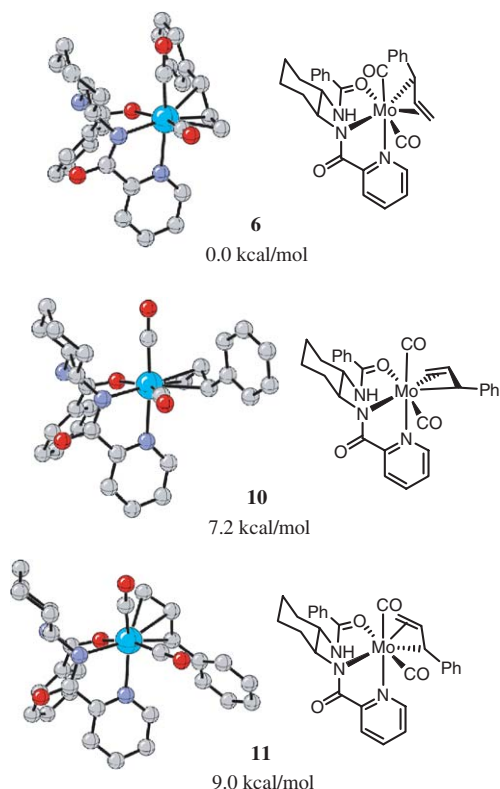


**Figure 8.** Calculated structures of rotamers of **6**. Isomer **6** is shown for reference.

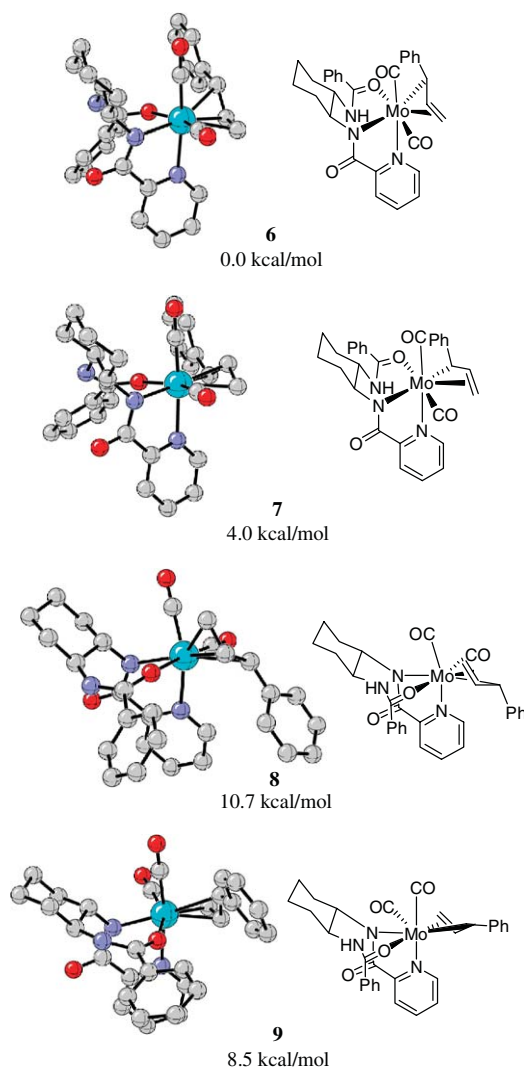


**Figure 9.** Stereoisomers of **6** formed via  $\pi$ – $\sigma$ – $\pi$  isomerization of the  $\pi$ -allyl group or dissociation, association of the chiral ligand. Isomer **6** is shown for reference.

in Table 2. As predicted, the (*R,R*)-isomer **7**, is 4.3 kcal/mol higher in energy than **6**, indicating a strong preference for binding the allyl ligand (*S,S*) rather than (*R,R*). Reorientation of the chiral ligand leads to less stable

**Table 2.** Relative energies of **7–9** rotamers

Isomer	Structure	Relative energy (kcal/mol)
<b>12</b>		4.3
<b>13</b>		9.1



isomers, whether the ligand is bound (*S,S*)-**8** (10.7 kcal/mol) or (*R,R*)-**9** (8.5 kcal/mol).

Steric interactions between the allyl group and the chiral ligand destabilize **7–9**. The effect of these steric interactions is most easily seen comparing **6** and **9**. Pseudo-enantiomers **6** and **9** have similar binding of the allyl ligand. Isomers **6** and **9** are pseudo-enantiomers since the stereochemistry of the chiral ligand does not change. Figure 10 shows **6** and **9** looking down the CO–Mo–pyridine axis. The chiral ligand orients the benzamide away from the  $\pi$ -allyl ligand in **6**. In **9**, the (*S,S*)-orientation places the benzamide group closer to the allyl ligand (3.47 Å vs 2.60 Å). The greater steric interaction in **9** causes it to be 8.5 kcal/mol higher in energy than its pseudo-enantiomer **6**.

The rotamers of **7–9** that lie within 10 kcal/mol of **6** are shown in Table 2. Six other rotamers of **7–9** were found and average 13.8 kcal/mol above **6**. Rotamers **12** and **13** are less stable due to increased overlap between the molybdenum pseudo- $d_{xy}$  orbital and the  $\pi$ -allyl orbital and destabilizing steric interactions.

Since molybdenum binds the chiral ligand facially, there are three possible locations for the allyl ligand. The crystal structure contains  $\pi$ -allyl group *trans* to the picolinamide nitrogen. Isomers with  $\pi$ -allyl *trans* to the benzamide oxygen and the pyridine nitrogen were investigated. Isomers with  $\pi$ -allyl bound (*R,R*) and (*S,S*) and the two orientations of the chiral ligand were investigated. The results are given in Figure 11 for the  $\pi$ -allyl *trans* to benzamide and Figure 12 for  $\pi$ -allyl *trans* to benzamide and Figure 12 for  $\pi$ -allyl *trans* to benzamide and Figure 12 for  $\pi$ -allyl *trans* to benzamide

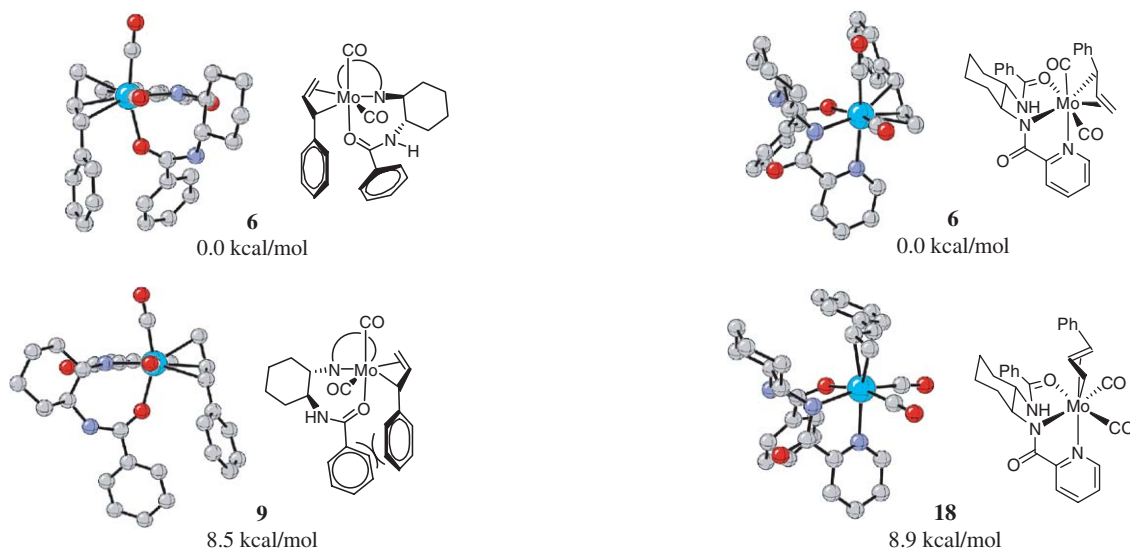


Figure 10. Pseudo-enantiomers **6** and **9** viewed down the axial carbonyl–molybdenum–pyridine bond.

Figure 12. Lowest energy isomer with allyl *trans* to pyridine, **18**. Isomer **6** is shown for reference.

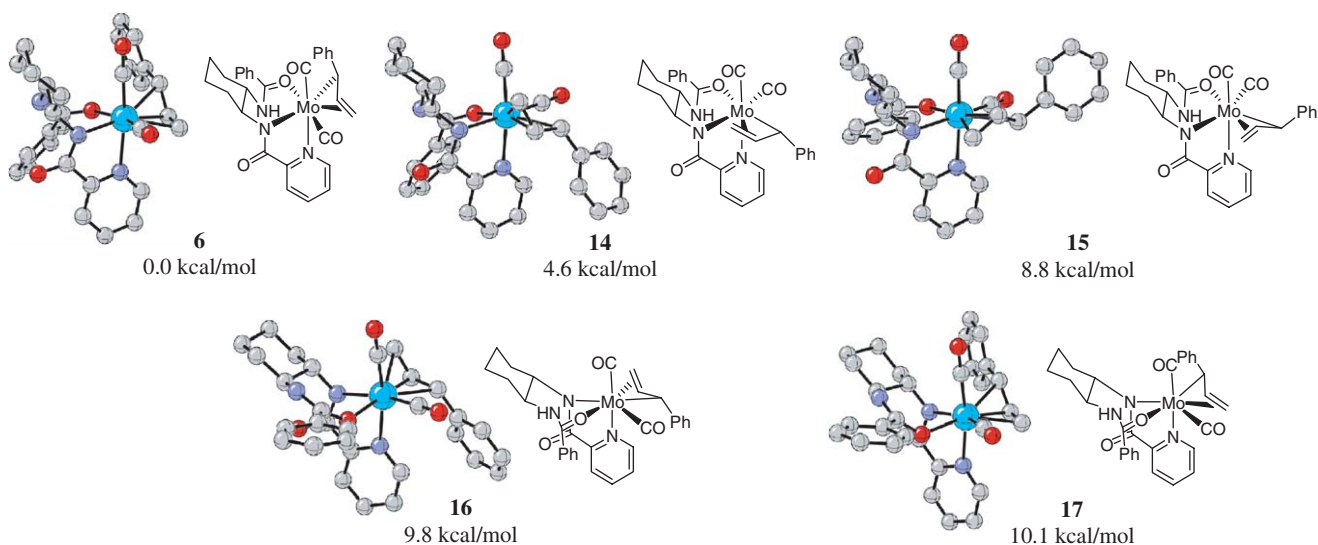
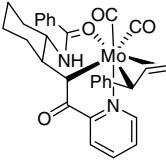


Figure 11. Isomers with allyl *trans* to benzamide, **14–17**. Isomer **6** is shown for reference.

pyridine. Rotamers within 10 kcal/mol of **6** are given in Table 3.

**Table 3.** Relative energies of **14–18** rotamers

Isomer	Structure	Relative energy (kcal/mol)
<b>19</b>		8.2

Allyl ligand *trans* to the benzamide oxygen results in isomers that are less stable than **6**, Figure 11. With the chiral ligand oriented as in **6**, the molybdenum center shows a slight preference for binding the allyl ligand (*S,S*)-**14** (4.6 kcal/mol) rather than (*R,R*)-**15** (8.6 kcal/mol). After dissociation–association of the chiral ligand, neither binding mode is favored. Isomer **14** is the most stable isomer (4.6 kcal/mol) with phenyl distal to the chiral ligand. Compounds **16** and **17** are least stable (9.8 and 10.1 kcal/mol, respectively).

It is noteworthy that the observed structure, **6**, gains stability by orientating the allyl group *trans* to picolinamide nitrogen. The interaction between the picolinamide lone pair and the molybdenum pseudo- $d_{xy}$  orbital increases the backbonding between the molybdenum and the allyl ligand and stabilizes **6**. Backbonding is not effected when allyl is *trans* to benzamide or pyridine. Isomers with the allyl *trans* to picolinamide are, on average, lower in energy than those with the allyl *trans* to the benzamide oxygen or the pyridine nitrogen.

The most stable rotamer with the allyl ligand *trans* to the pyridine nitrogen is shown in Figure 12. Isomers with the allyl ligand *trans* to pyridine are the least stable with average energies of 17.1 kcal/mol (vs 10.3 for allyl *trans* to picolinamide and 11.4 kcal/mol for allyl *trans* to benzamide). In fact, only **18** lies within 10 kcal/mol of **6**.

Again, isomers with allyl *trans* to pyridine are not as stable as those with allyl *trans* to picolinamide since the pyridine nitrogen is only a  $\sigma$  donor ligand. A  $\sigma$  donor cannot interact with the filled, orthogonal molybdenum orbitals and cannot increase backbonding within the complex. These isomers are further destabilized by increased steric interactions between the allyl ligand and the cyclohexyl of the chiral ligand.

### 3. Conclusion

The stability of **6** has been analyzed. Geometric isomers, diastereomers, and  $\pi$ -allyl rotamers were calculated and found to be less stable than the observed **6**. The stability of **6** is due to a combination of electronic and steric factors. The allyl *trans* to picolinamide stabilizes **6** by increasing the ability of the  $d_{xy}$  orbital to backbond with

the allyl ligand. The observed orientation of the chiral ligand places the benzamide phenyl ring out of the equatorial plane. The phenyl ring of the allyl group is distal to the chiral ligand and the  $\pi$  orbitals of the carbonyl ligands, minimizing these destabilizing steric and electronic interactions. The allyl ligand bound (*S,S*), rather than (*R,R*), also minimizes these interactions. Isomer **6** orients the open face of the  $\pi$ -allyl complex toward the two carbonyl ligands, minimizing the interaction between the filled molybdenum pseudo- $d_{xy}$  orbital and the filled allyl orbital.

We have established that the observed intermediate is computationally the most stable. The mechanism by which **6** interacts with the nucleophile to generate the branched product with net retention of configuration at the alpha carbon is the focus of the ongoing computational study.

### 4. Computational details

Calculations were performed using Gaussian 03.<sup>19</sup> Initial geometry optimizations were performed using HF/3-21G\*. Subsequent geometry optimizations were performed with the B3LYP functional<sup>20</sup> with the 6-31G\* basis set<sup>21</sup> for all atoms except Mo, for which the LANL2DZ+ECP<sup>22</sup> basis set was used. Frequency calculations were performed at B3LYP/3-21G\*+LANL2DZ to confirm each stationary point as a local minimum.

### Acknowledgments

We are grateful to the National Institute of General Medical Sciences, National Institutes of Health, for financial support of this research. We also thank the National Computational Science Alliance (NCSA) and UCLA Academic Technology Services for computing resources.

### References

- (a) Trost, B. M. *J. Org. Chem.* **2004**, *69*, 5813–5837; (b) Trost, B. M.; Crawley, M. L. *Chem. Rev.* **2003**, *103*, 2921–2944; (c) Trost, B. M.; Van Vranken, D. L. *Chem. Rev.* **1996**, *96*, 395–422.
- (a) Pfaltz, A.; Lautens, M. *Compr. Asymmetric Catal.* **1999**, *2*, 833–884; (b) Trost, B. M. *Acc. Chem. Res.* **1996**, *29*, 355–364; (c) Frost, C. G.; Howarth, J.; Williams, J. M. *J. Tetrahedron: Asymmetry* **1992**, *3*, 1089–1122; (d) Helmchen, G.; Kudis, S.; Sennhenn, P.; Steinhagen, H. *Pure Appl. Chem.* **1997**, *69*, 336–345.
- Ru: (a) Trost, B. M.; Fraisse, P.; Ball, Z. T. *Angew. Chem., Int. Ed.* **2002**, *41*, 1059–1061; (b) Morisaki, Y.; Kondo, T.; Mitsudo, T. *Organometallics* **1999**, *18*, 4742–4746; (c) Zhang, S. W.; Mitsudo, T.; Kondo, T.; Watanabe, Y. *J. Organomet. Chem.* **1993**, *450*, 197–207; Rh: (d) Hayashi, T.; Okada, A.; Suzuka, T.; Kawatsura, M. *Org. Lett.* **2003**, *5*, 1713–1715; (e) Evans, P. A.; Kennedy, L. J. *J. Am. Chem. Soc.* **2001**, *123*, 1234–1235; (f) Evans, P. A.; Nelson, J. D. *J. Am. Chem. Soc.* **1998**, *120*, 5581–5582; Ir: (g) Lipowsky, G.; Miller, N.; Helmchen, G. *Angew.*

- Chem., Int. Ed.* **2004**, *43*, 4595–4597; (h) Bartels, B.; Garcia-Yebra, C.; Rominger, F.; Helmchen, G. *Eur. J. Inorg. Chem.* **2002**, 2569–2586; (i) Takeuchi, R.; Ve, N.; Tanabe, K.; Yamashita, K.; Shiga, N. *J. Am. Chem. Soc.* **2001**, *123*, 9525–9534; (j) Bartels, B.; Helmchen, G. *Chem. Commun.* **1999**, 741–742; (k) Takeuchi, R.; Kashio, M. *J. Am. Chem. Soc.* **1998**, *120*, 8647–8655; (l) Janssen, J. P.; Helmchen, G. *Tetrahedron Lett.* **1997**, *38*, 8025–8026; Fe: (m) Eberhardt, U.; Mattern, G. *Chem. Ber.* **1988**, *121*, 1531–1534; (n) Xu, Y.; Zhou, B. *J. Org. Chem.* **1987**, *52*, 974–977; W: (o) Lehmann, J.; Lloyd-Jones, G. C. *Tetrahedron* **1995**, *51*, 8863–8874.
4. (a) Trost, B. M.; Dogra, K.; Hachiya, I.; Emura, T.; Hughes, D. L.; Krska, S.; Reamer, R. A.; Palucki, M.; Yasuda, N.; Reider, P. J. *Angew. Chem., Int. Ed.* **2002**, *41*, 1929–1932; (b) Hughes, D. L.; Palucki, M.; Yasuda, N.; Reamer, R. A.; Reider, P. J. *J. Org. Chem.* **2002**, *67*, 2762–2768; (c) Malkov, A. V.; Spoor, P.; Vinader, V.; Kočovský, P. *Tetrahedron Lett.* **2001**, *42*, 509–512; (d) Kaiser, N.-F. K.; Bremberg, U.; Larhed, M.; Moberg, C.; Hallberg, A. *Angew. Chem., Int. Ed.* **2000**, *39*, 3595–3598; (e) Glorius, F.; Pfaltz, A. *Org. Lett.* **1999**, *1*, 141–144; (f) Kočovský, P.; Malkov, A. V.; Vyskočil, A.; Lloyd-Jones, G. C. *Pure Appl. Chem.* **1999**, *71*, 1425–1433; (g) Lloyd-Jones, G. C.; Pfaltz, A. *Angew. Chem., Int. Ed. Engl.* **1995**, *34*, 462–464; (h) Trost, B. M.; Merlic, C. A. *J. Am. Chem. Soc.* **1990**, *112*, 9590–9600; (i) Faller, J. W.; Chao, K.-H. *J. Am. Chem. Soc.* **1983**, *105*, 3893–3898; (j) Trost, B. M.; Lautens, M. J. *Am. Chem. Soc.* **1982**, *104*, 5543–5545; (k) Adams, R. D.; Chodosh, D. F.; Faller, J. W.; Rosan, A. M. *J. Am. Chem. Soc.* **1979**, *101*, 2570–2578.
  5. (a) Lloyd-Jones, G. C.; Krska, S. W.; Hughes, D. L.; Gouriou, L.; Bonnet, V. D.; Jack, K.; Sun, Y.; Reamer, R. A. *J. Am. Chem. Soc.* **2004**, *126*, 702–703; (b) Hughes, D. L.; Lloyd-Jones, G. C.; Krska, S. W.; Gouriou, L.; Bonnet, V. D.; Jack, K.; Sun, Y.; Mathre, D. J.; Reamer, R. A. *Proc. Natl. Acad. Sci. U.S.A.* **2004**, *101*, 5379–5384.
  6. Krska, S. W.; Hughes, D. L.; Reamer, R. A.; Mathre, D. J.; Sun, Y. *J. Am. Chem. Soc.* **2002**, *124*, 12656–12657.
  7. A minor allyl complex (~1%) was observed with <sup>1</sup>H NMR. This minor complex is in dynamic equilibrium with **6** according to spin saturation transfer experiments. However, the minor complex is not related to **6** via  $\pi$ - $\sigma$ - $\pi$  isomerization, indicating it is either a rotamer of **6** or perhaps **7**. Krska, S. W.; Hughes, D. L.; Reamer, R. A.; Mathre, D. J.; Palucki, M.; Yasuda, N.; Sun, Y.; Trost, B. M. *Pure Appl. Chem.* **2004**, *76*, 625–633.
  8. (a) Chan, A. S. C.; Pluth, J. J.; Halpern, J. *J. Am. Chem. Soc.* **1980**, *102*, 5952–5954; (b) Chua, P. S.; Roberts, N. K.; Bosnich, B.; Okrasinski, S. J.; Halpern, J. *J. Chem. Soc., Chem. Commun.* **1981**, 1278–1280; (c) Landis, C. R.; Halpern, J. *J. Am. Chem. Soc.* **1987**, *109*, 1746–1754; (d) Feldgus, S.; Landis, C. R. *J. Am. Chem. Soc.* **2000**, *122*, 12714–12727; (e) Halpern, J. *Pure Appl. Chem.* **2001**, *73*, 209–220; (f) Nettekoven, U.; Hartwig, J. F. *J. Am. Chem. Soc.* **2002**, *124*, 1166–1167; (g) Schmidt, T.; Baumann, W.; Drexler, H.-J.; Arrieta, A.; Heller, D.; Buschmann, H. *Organometallics* **2005**, *24*, 3842–3848.
  9. (a) Merlic, C. A.; Miller, M. M.; Hietbrink, B. N.; Houk, K. N. *J. Am. Chem. Soc.* **2001**, *123*, 4904–4918; (b) Tantillo, D. J.; Hietbrink, B. N.; Merlic, C. A.; Houk, K. N. *J. Am. Chem. Soc.* **2000**, *122*, 7136–7137; (c) Merlic, C. A.; Walsh, J. C.; Tantillo, D. J.; Houk, K. N. *J. Am. Chem. Soc.* **1999**, *121*, 3596–3606; (d) Jemmis, E. D.; Gijju, K. T. *J. Am. Chem. Soc.* **1998**, *120*, 6952–6964; (e) Decker, S. A.; Klobukowski, M. *J. Am. Chem. Soc.* **1998**, *120*, 9342–9355.
  10. Nemykin, V. N.; Basu, P. *Inorg. Chem.* **2003**, *42*, 4046–4056.
  11. Cotton, F. A.; Luck, R. L. *Acta Crystallogr.* **1990**, *C46*, 138–140.
  12. (a) Drew, M. G. B.; Brisdon, B. J.; Brown, D. W.; Willis, C. R. *J. Chem. Soc., Chem. Commun.* **1986**, 1510–1512; (b) Lee, G.-H.; Peng, S.-M.; Liu, F.-C.; Mu, D.; Liu, R.-S. *Organometallics* **1989**, *8*, 402–407; (c) Pax-Sandoval, M. A.; Saavedra, F. J.; Pomposo, G. D.; Joseph-Nathan, P.; Powell, P. J. *Organomet. Chem.* **1990**, *387*, 265–276; (d) Wu, S. L.; Cheng, C.-Y.; Wang, S.-L.; Liu, R.-S. *Inorg. Chem.* **1991**, *30*, 311–316.
  13. (a) Graham, A. J.; Fenn, R. H. *J. Organomet. Chem.* **1969**, *17*, 405–422; (b) Graham, A. J.; Fenn, R. H. *J. Organomet. Chem.* **1970**, *25*, 173–191; (c) Kosky, C. A.; Ganis, P.; Avitabile, G. *Acta Crystallogr.* **1971**, *B27*, 1859–1864; (d) Cotton, F. A.; Frenz, B. A.; Stanislawski, A. G. *Inorg. Chim. Acta* **1973**, *7*, 503–508; (e) Dawans, F.; Dewailly, J.; Meunier-Piret, J.; Piret, P. *J. Organomet. Chem.* **1974**, *76*, 53–63; (f) Brisdon, B. J.; Woolf, A. A. *J. C. S. Dalton* **1978**, 291–295; (g) Drew, M. G. B.; Brisdon, B. J.; Cartwright, M. *Inorg. Chim. Acta* **1979**, *36*, 127–133; (h) Graham, A. J.; Akrigg, D.; Sheldrick, B. *Acta Crystallogr.* **1983**, *C39*, 192–194; (i) Graham, A. J.; Akrigg, D.; Sheldrick, B. *Acta Crystallogr.* **1985**, *C41*, 995–996; (j) Gracey, G. D.; Rettig, S. J.; Storr, A.; Trotter, J. *Can. J. Chem.* **1987**, *65*, 2469–2477; (k) Jordanov, J.; Behm, H.; Beurskens, P. T. *J. Crystallogr. Spectrosc. Res.* **1991**, *21*, 657–659; (l) Shiu, K.-B.; Chang, C.-J.; Wang, S.-L.; Liao, F.-L. *J. Organomet. Chem.* **1991**, *407*, 225–235; (m) Miguel, D.; Pérez-Martínez, J. A.; Riera, V. *Organometallics* **1994**, *13*, 1336–1340; (n) Espinet, P.; Hernandez, R.; Iturbe, G.; Villafañe, F.; Orpen, A. G.; Pascual, I. *Eur. J. Inorg. Chem.* **2000**, 1031–1038.
  14. (a) Albright, T. A.; Burdett, J. K.; Whangbo, M.-H. *Orbital Interactions in Chemistry*; Wiley: New York, 1985, Chapter 14; (b) Miessler, G. L.; Tarr, D. A. *Inorganic Chemistry*, 2nd ed.; Prentice Hall: Upper Saddle River, NJ, 1999, pp 319–329.
  15. (a) Curtis, M. D.; Eisenstein, O. *Organometallics* **1984**, *3*, 887–895; (b) Curtis, M. D.; Fotinos, N. A. *J. Organomet. Chem.* **1984**, *272*, 43–54.
  16. (a) Gunnoe, T. B.; Sabat, M.; Harman, W. D. *Organometallics* **2000**, *19*, 728–740; (b) Gunnoe, T. B.; Sabat, M.; Harman, W. D. *J. Am. Chem. Soc.* **1999**, *121*, 6449–6500.
  17. Drew, M. G. B.; Brisdon, B. J.; Edwards, D. A.; Paddick, K. E. *Inorg. Chim. Acta* **1979**, *35*, L381–L382.
  18. (a) Sjögren, M. P. T.; Frisell, H.; Åkermark, B.; Norrby, P.-O.; Eriksson, L.; Vitagliano, A. *Organometallics* **1997**, *16*, 942–950; (b) Ascenso, J. R.; de Azevedo, C. G.; Calhorda, M. J.; Carrondo, M. A. A. F. de C. T.; Costa, P.; Dias, A. R.; Dreq, M. G. B.; Félix, V.; Galvão, A. M.; Romão, C. C. *J. Organomet. Chem.* **2001**, *632*, 197–208.
  19. Frisch, M. J.; Trucks, G. W.; Schlegel, H. B.; Scuseria, G. E.; Robb, M. A.; Cheeseman, J. R.; Montgomery, J. A., Jr.; Vreven, T.; Kudin, K. N.; Burant, J. C.; Millam, J. M.; Iyengar, S. S.; Tomasi, J.; Barone, V.; Mennucci, B.; Cossi, M.; Scalmani, G.; Rega, N.; Petersson, G. A.; Nakatsuji, H.; Hada, M.; Ehara, M.; Toyota, K.; Fukuda, R.; Hasegawa, J.; Ishida, M.; Nakajima, T.; Honda, Y.; Kitao, O.; Nakai, H.; Klene, M.; Li, X.; Knox, J. E.; Hratchian, H. P.; Cross, J. B.; Adamo, C.; Jaramillo, J.; Gomperts, R.; Stratmann, R. E.; Yazyev, O.; Austin, A. J.; Cammi, R.; Pomelli, C.; Ochterski, J. W.; Ayala, P. Y.; Morokuma, K.; Voth, G. A.; Salvador, P.; Dannenberg, J. J.; Zakrzewski, V. G.; Dapprich, S.; Daniels, A. D.; Strain, M. C.; Farkas, O.; Malick, D. K.; Rabuck, A. D.; Raghavachari, K.; Foresman, J. B.; Ortiz, J. V.; Cui, Q.; Baboul, A. G.; Clifford, S.; Cioslowski, J.; Stefanov, B. B.; Liu, G.; Liashenko, A.; Piskorz, P.; Komaromi, I.; Martin, R. L.; Fox, D. J.; Keith, T.; Al-Laham, M. A.;



- Peng, C. Y.; Nanayakkara, A.; Challacombe, M.; Gill, P. M. W.; Johnson, B.; Chen, W.; Wong, M. W.; Gonzalez, C.; Pople, J. A. *Gaussian 03, Revision B.05*; Gaussian: Pittsburgh, PA, 2003.
20. (a) Becke, A. D. *J. Chem. Phys.* **1993**, *98*, 5648–5652; (b) Lee, C.; Yang, W.; Parr, R. G. *Phys. Rev. B* **1988**, *37*, 785–789; (c) Ditchfield, R.; Hehre, W. J.; Pople, J. A. *J. Chem. Phys.* **1971**, *54*, 724–728; (d) Hehre, W. J.; Ditchfield, R.; Pople, J. A. *J. Chem. Phys.* **1972**, *56*, 2257–2261.
21. Hariharan, P. C.; Pople, J. A. *Theor. Chim. Acta* **1973**, *28*, 213.
22. Wadt, W. R.; Hay, P. J. *J. Chem. Phys.* **1985**, *82*, 284–298.